WATER RESOURCES RESEARCH, VOL. 35, NO. 8, PAGES 2347–2358, AUGUST 1999

Modeling groundwater with ocean and river interaction

G. Carabin and A. Dassargues[1]

Laboratoires de Géologie de l'Ingénieur, d'Hydrogéologie, et de Prospection Géophysique, Université de Liège Liege, Belgium

Abstract. We develop and implement the groundwater model, Saturated/Unsaturated Flow and Transport in 3D (SUFT3D), to integrate water quantity/quality data and simulations with models of other hydrologic cycle components, namely, rivers and the ocean. This work was done as part of the Sea Air Land Modeling Operational Network (SALMON) project supported by the IBM International Foundation through its Environmental Research Program. The first research steps, presented here, address the simulation of typical hydrologic conditions to demonstrate SUFT3D's effectiveness and accuracy. The theory behind the modeling of seawater intrusion and groundwater-river interaction is summarized along with the numerical methods and characteristics of SUFT3D. The code was applied to different, increasingly complex scenarios: confined to unconfined conditions, local to regional scale, homogeneous to increasing heterogeneity, two- to three-dimensional. Of particular interest were the impacts of different boundary conditions and influence of river interactions on seawater intrusion. Results are illustrated, discussed, and compared, when possible, to those in the literature. Simulating groundwater exchange between both the river and the ocean has provided interesting results that better depict the dynamics of flow and transport in coastal zone groundwater systems.

1. Introduction

Different models can be developed to simulate water flow and quality at large scales in both time and space. Each part of the hydrological cycle, i.e., ocean, surface water, groundwater, and atmosphere, is simulated using models adapted to each particular component. Usually, each model is designed for only one part of the water cycle, and interactions with other parts are taken into account by using prescribed input/output flux at the boundaries. This is commonly considered as satisfactory so that groundwater, river, and ocean models are usually connected only by these prescribed boundary conditions. However, the actual water and contaminant fluxes between the models should be simulated more realistically without prescribing any flux. Integrated water quantity and quality problems in coastal zones were investigated as part of the Sea Air Land Modeling Operational Network (SALMON) project supported by the IBM International Foundation. This research focuses on introducing natural "junctions" between the different models to adequately compute exchange flux. As of 1995, three models (ocean [*Beckers*, 1991], river [*Smitz et al.*, 1997], and groundwater [*Dassargues*, 1994]) had been developed in different departments of the University of Liège. Now, these are being connected to form an integrated model, able to describe water and contaminant flux over the entire system at regional scales, including input from marine, river, groundwater, and atmospheric hydrologic cycle components.

Connecting the different models is done through a specific interface, called a junction, designed to manage data exchange between models. On the basis of different numerical methods, these models each have independent time and space discretization. The data exchange must be organized by the junction using various time and space interpolations schemes. These developments are introduced taking advantage of distributed memory parallel architecture (an IBM Risc/6000 Scaleable Powerparallel (SP2) system), and the Parallel Virtual Machine (PVM) software is used for the data exchange management between the tasks running on the different processors. Details on the data exchange organization via the junction are given by *Dassargues et al.* [1996].

For groundwater the first research step was to develop the Saturated Unsaturated Flow and Transport in 3D (SUFT3D) groundwater model and to check its effectiveness and accuracy to reproduce typical situations of seawater intrusion and then groundwater-river interactions influenced by seawater intrusion. Results of these tests with interactions involving only groundwater are documented below.

2. Interactions With the Ocean Model: Theoretical Background

In coastal zones, salt water greatly influences groundwater flow and quality. This well-documented effect, seawater intrusion, is caused by the density difference between salt and fresh water. Groundwater quality degradation is extensive in many coastal aquifers as the result of contamination by salt water where an "upconing" phenomenon is induced near large-scale pumping wells.

For more than 20 years, many authors have studied how to develop groundwater numerical codes to simulate seawater intrusion problems. Two very different conceptual models have been developed: (1) no mixing zone, a sharp interface between salt and fresh water, (2) a transition or mixing zone, a gradient between salt and fresh water. *Galeati et al.* [1992] listed many authors [*Liu et al.*, 1981; *Huyakorn and Pinder*, 1983; *Taigbenu et al.*, 1984; *Voss and Souza*, 1987; *Essaid*, 1990] who studied seawater intrusion problems between 1977 and 1990. They

[1]Also at Hydrogeologie, Afdeling Historische Geologie, Departement Geografie-Geologie, Katholieke Universiteit Leuven, Leuven, Belgium.

Paper number 1999WR900127.
0043-1397/99/1999WR900127$09.00

presented analytical or numerical solutions of relatively easy two-dimensional (2-D) problems using the first or the second model concepts and numerical solutions of 3-D problems using only the second, mixing zone model. Now, 3-D examples of the sharp interface exist [*Larabi and De Smedt*, 1994]. However, it is generally agreed that a mixing zone should be taken into account in two or three dimensions when dispersion or a vertical flow component becomes important in the aquifer. We have adopted the mixing zone model to study different actual 3-D cases where heterogeneity and dispersion cannot be neglected.

In a transition zone the fluid (water) density may vary in space and time as a function of changes in concentration, temperature, and pressure. This leads to coupled or partially coupled groundwater flow and transport equations with nonlinear parameters. The equations implemented in groundwater codes are usually derived from basic principles of conservation of mass (written for water and solutes) and linear momentum with associated constitutive equations. More generally coupled equations containing cross-coupling terms can be derived from a rigorous thermodynamic approach [*Hassanizadeh and Leijnse*, 1988], but this is only pertinent to cases of high salt concentration (proximity to salt domes or salt formations). In our study the classical approach of balanced equations expressed for a unit volume of porous medium was used, as summarized below.

The averaged momentum balance equation can be reduced to the linear Darcy's law for an aquifer. This is appropriate when there are isothermal, saturated conditions and with classical assumptions concerning the solid-fluid interactions, negligible internal friction in the fluid, and negligible inertial effects, as developed by *Bear and Bachmat* [1990], and is expressed as

$$\mathbf{v} = -\frac{\mathsf{k}}{n\mu}\left[\text{grad}\ (p) + \rho g\ \text{grad}(z)\right] \tag{1}$$

with

- $\mathbf{v}$ averaged effective velocity vector $[L/T]$;
- n effective porosity or 'mobile' water porosity [dimensionless];
- k intrinsic permeability tensor $[L^2]$;
- μ fluid viscosity $[M(LT)^{-1}]$;
- ρ fluid density $[M/L^3]$;
- g acceleration due to gravity $[L/T^2]$;
- p fluid pressure $[M/LT^2]$;

where all variables or parameters are considered at a macroscopic scale using representative elementary volume (REV) theory associated with a continuum approach and porous medium concept.

The mass balance equation for water is generally expressed as [e.g., *Yeh*, 1993]

$$\frac{\partial(nS\rho)}{\partial t} = -\text{div}\ (nS\rho\mathbf{v}) - \text{div}\ (nS\rho\mathbf{V}_s) + \rho^* q \tag{2}$$

where

- S degree of saturation [dimensionless];
- $\mathbf{V}_s$ velocity of the deformable surface $[L/T]$;
- q internal sink/source flow rate $[L^3/TL^3]$;
- ρ^* fluid density in the sink/source term $[M/L^3]$.

If $q > 0$, then $\rho^* = \rho^*$ (prescribed by the external fluid source), and if $q < 0$, then $\rho^* = \rho$. In the unsaturated zone (1) for averaged effective velocity must be divided by the degree of saturation (S). In addition, intrinsic permeability depends on S.

The left side of (2) expresses the time variation of the storage of the fluid in the porous medium. If isothermal conditions are assumed,

$$\frac{\partial}{\partial t}(nS\rho) = \rho S\frac{\partial n}{\partial t} + \rho n\frac{\partial S}{\partial t} + nS\frac{\partial \rho}{\partial p}\frac{\partial p}{\partial t} + nS\frac{\partial \rho}{\partial C}\frac{\partial C}{\partial t} \tag{3}$$

where C is the solute mass fraction $[M/M]$ or solute concentration $[M/L^3]$. We define water content θ [dimensionless] by

$$\theta = nS \tag{4}$$

and coefficient of fluid compressibility at constant temperature and concentration, β $[LT^2/M]$, by

$$\beta = \frac{1}{\rho}\frac{\partial \rho}{\partial p} \tag{5}$$

Using the mass balance equation for an incompressible solid (but a compressible skeleton) with the definition of the volumetric compressibility coefficient of a porous medium, α $[LT^2/M]$, yields

$$\text{div}\ (\mathbf{V}_s) = \alpha\frac{\partial p}{\partial t} \tag{6}$$

Then, (2) becomes

$$\rho(\theta\beta + S\alpha)\frac{\partial p}{\partial t} + \rho n\frac{\partial S}{\partial t} + nS\frac{\partial \rho}{\partial C}\frac{\partial C}{\partial t} = \text{div}\left\{\frac{\rho\mathsf{k}}{\mu}\left[\text{grad}\ (p) + \rho g\ \text{grad}\ (z)\right]\right\} + \rho^* q \tag{7}$$

The transient term due to variation in saturation degree can be expressed as a function of pressure p using the concept of specific water capacity, $d\theta/d\psi$ $[L^{-1}]$ [*Hillel*, 1984], where ψ is the pressure head.

Consequently the mass balance equation for water can be written in terms of the two main dependent variables, p and C, as

$$\rho\left(\theta\beta + \frac{\theta}{n}\alpha\right)\frac{\partial p}{\partial t} + \frac{1}{g}\frac{d\theta}{d\psi}\frac{\partial p}{\partial t} + \theta\frac{\partial \rho}{\partial C}\frac{\partial C}{\partial t} = \text{div}\left\{\frac{\rho\mathsf{k}}{\mu}\left[\text{grad}\ (p) + \rho g\ \text{grad}\ (z)\right]\right\} + \rho^* q \tag{8}$$

or in terms of C and reference pressure head, $h = p/\rho_0 g$ (with ρ_0 a reference water density),

$$\frac{\rho}{\rho_0}\left(\theta\rho_0 g\beta + \frac{\theta}{n}\rho_0 g\alpha + \frac{d\theta}{dh}\right)\frac{\partial h}{\partial t} + \frac{\theta}{\rho_0}\frac{\partial \rho}{\partial C}\frac{\partial C}{\partial t} = \text{div}\left\{\frac{\rho g\mathsf{k}}{\mu}\left[\text{grad}\ (h) + \frac{\rho}{\rho_0}\text{grad}\ (z)\right]\right\} + \frac{\rho^*}{\rho_0}q \tag{9}$$

The solute mass balance equation or transport equation can be expressed in the traditional way [e.g., *Bear and Verruijt*, 1987; *Kinzelbach*, 1986; *Kipp*, 1987], generalized for the unsaturated zone as

$$\frac{\partial(\theta\rho C)}{\partial t} = -\text{div}\ (\theta\rho C\mathbf{v}) - \text{div}\ (\theta\rho C\mathbf{V}_s) + \text{div}\ [\theta\rho(\mathsf{D} + D_m\mathsf{I})\ \text{grad}\ (C)] + \rho^* q C^* \tag{10}$$

where the processes of adsorption/desorption, decay, and immobile water effect are neglected and where D is mechanical dispersion tensor (dependent on effective velocity) $[L^2/T]$, D_m is effective molecular diffusion coefficient of solute in porous media $[L^2/T]$, and C^* is fluid concentration (mass fraction) in sink/source term (equal to C if $q \leq 0$) $[M/M]$. Variations of fluid density and viscosity with solute concentration are usually expressed by polynomial or exponential expressions. In cases of moderately salty water the fluid density constitutive equation can be reduced to a linear form as

$$\rho = \rho_0[1 + \beta_C(C - C_0)] \tag{11}$$

with

$$\beta_C = \frac{1}{\rho_0}\left(\frac{\partial \rho}{\partial C}\right)_{p,T\,\mathrm{cst}}$$

Using relative concentration C_r defined by $C_r = (C - C_{\min})/(C_{\max} - C_{\min})$ with $C_{\min} = C_0$, (11) can be written

$$\frac{\rho}{\rho_0} = 1 + \varepsilon C_r \tag{12}$$

with

$$\varepsilon = \frac{\rho_{\max}}{\rho_0} - 1$$

Equations (8) and (10) are mainly coupled taking into consideration that variation of density as a function of concentration $\rho(C)$ will influence groundwater flow effective velocity, $\mathbf{v}$ (equation (1)), in a way which renders both (8) and (10) nonlinear.

Many authors [e.g., *Gartling and Hickox*, 1985; *Hassanizadeh and Leijnse*, 1988; *Galeati et al.*, 1992] do not consider the system of (8) and (10) in their total complexity. They use an approximation known as the Boussinesq approximation, and additionally, they are not interested in the partially saturated zone. The Boussinesq approximation states that density variation is to be considered only in the Darcy's law equation (1), reducing the water mass balance equation (9) to a volumetric balance equation:

$$(\rho_0 g\alpha)\frac{\partial h}{\partial t} = \mathrm{div}\left\{\frac{\rho(C)g\mathsf{k}}{\mu(C)}\left[\mathrm{grad}\,(h) + \frac{\rho(C)}{\rho_0}\mathrm{grad}\,(z)\right]\right\} + \frac{\rho^*}{\rho_0}q \tag{13}$$

In terms of equivalent freshwater piezometric head, $(H = h + z = (p/\rho_0 g) + z)$, using (12), we obtain

$$(\rho_0 g\alpha)\frac{\partial H}{\partial t} = \mathrm{div}\mathsf{K}'[\mathrm{grad}\,(H) + \varepsilon C_r\,\mathrm{grad}\,(z)] + \frac{\rho^*}{\rho_0}q \tag{14}$$

with $\mathsf{K}' = \mathsf{k}\rho(C)g/\mu(C)$, the "modified" tensor of hydraulic conductivity.

Equation (14) shows that when dealing with nonideal solutes, fluid flux is not orthogonal to equipotential lines. Using this system is generally qualified, in the literature, as adopting the "generalized Boussinesq approximation." Moreover, if K' is assumed constant with regard to solute concentration, one generally speaks of the "classical Boussinesq approximation."

On the basis of error analysis, *Munhoven* [1992] showed that this last approximation can be accepted when expected salinity variations are limited to 5% (more than the usual contrast between freshwater and seawater) under pressure variations not exceeding 3.0×10^8 Pa (~3000 atm).

If additionally assumed that the porous medium is incompressible, the flow equation obtained for a confined aquifer is similar to the Laplace equation:

$$\mathrm{div}\,\mathsf{K}'[\mathrm{grad}\,(p) + \rho(C)g\,\mathrm{grad}\,(z)] + \rho^* gq = 0 \tag{15}$$

and the coupled transport equation is written

$$\frac{\partial C}{\partial t} = -\mathrm{div}(C\mathbf{v}) + \mathrm{div}\,[(\mathsf{D} + D_m\mathsf{I})\,\mathrm{grad}\,(C)] + \rho^* C^* q' \tag{16}$$

where $q' = q/n\rho_0$ is the modified sink/source term. As equations of this system are coupled, (15) can, however, still be considered as a transient equation due to time variation of solute concentration.

Applying this system of coupled flow-transport equations (with different simplifications) to an actual case requires knowledge of the characteristics of the coastal aquifers (e.g., geometry, groundwater flow and transport parameters) and the external influences (sink/source terms for flow and transport) commonly imposed or influenced by human activities. Moreover, for the 2-D ocean-groundwater interface (i.e., the shelf), two important variables, water pressure and seawater salt concentration, have to be known at each time step since they influence the extent of seawater intrusion.

For the SALMON project the models are run in parallel, and the data exchange (water pressure and salt concentration at the ocean-groundwater interface) through the junction allows the groundwater model (GWM) to solve for flow and salt transport taking into account seawater level fluctuations and evolution of saltwater concentrations from the ocean model (OM). Salt concentration can vary considerably near a river mouth. For the OM, interactions are supposedly too weak to influence the ocean hydraulics, but exchange of a solute should be taken into account at the interface. Consequently, water fluxes and concentrations calculated in the GWM are sent to the junction.

3. Interactions With the River Model: Theoretical Background

Exchange occurs between rivers and aquifers along their entire intersection length. Aquifers can be drained or recharged by the river according to their juxtaposition, as well as climate and seasonal conditions. The classical way to represent this interaction in groundwater modeling is straightforward. One of the two following groundwater flow boundary conditions is adopted: (1) a Dirichlet boundary condition or boundary condition of the first kind or (2) a Fourier boundary condition or boundary condition of the third kind. For Dirichlet boundary conditions, total head values H_g are prescribed equal to the elevation of the water level in the river (H_r):

$$H_g = H_r \tag{17}$$

With Fourier boundary conditions the river exchange flux q is computed depending on the difference between aquifer piezometric head and river water level:

$$q = \frac{K_r}{e_r}(H_g - H_r) \tag{18}$$

where K_r is hydraulic conductivity $[L/T]$ and e_r is thickness $[L]$ of the river bottom or bank. The ratio K_r/e_r defines a water transfer leakage coefficient between the aquifer and river.

The choice of boundary conditions is usually guided by the characteristics of the contact between the aquifer and river. *Bear and Verruijt* [1987] suggest using a Dirichlet boundary when the porous medium flow domain is in contact with a body of open water as long as the river bottom sediments are not an effective hydraulic barrier between the two domains. When a semipervious interface does exist, they suggest using the Fourier boundary. For the river-aquifer interface, low-permeability alluvium in the streambed could constitute a real semipervious layer. This Fourier condition can be used over the whole length of the water course even if this low-permeability layer is not continuously present [*McDonald and Harbaugh*, 1988; *Nawalany*, 1994]. In this case, K_r/e_r is assigned a high value so that there is no significant difference between the aquifer head and river water level at those places. Further, Fourier boundaries allow representative conditions to be simulated where the aquifer piezometric head can be below the river bottom, a condition not possible with Dirichlet conditions. When aquifer water levels fall below the river bottom, the groundwater head is replaced automatically by the river bottom level l_{rb} in (18):

$$q = \frac{K_r}{e_r}(l_{rb} - H_r) \tag{19}$$

For the SALMON project the Fourier boundary condition expressed by (18) and (19) has been chosen. By doing this it is possible to directly obtain an evaluation of the exchange flux in each finite element with such a boundary. It is also the more general and appropriate method to simulate actual river water level and aquifer fluctuations. However, the Fourier condition needs the ratio K_r/e_r to be known and introduced in each affected finite element. In SUFT3D the Fourier condition was implemented so that the boundary edge as well as boundary element side conditions could be prescribed. In this way, flexibility was introduced to accommodate rivers of variable widths. Consequently, the river model (RM)–groundwater model interface can be 1-D or 2-D.

At the interface the data exchange is organized at each time step. Organization of the exchanges as presented by *Dassargues et al.* [1996] was the following: (1) computed water levels and solute contaminants concentrations are sent by both models (GWM and RM) to the junction, and (2) after spatial and time interpolations the junction feeds calculated water flux (equation (18) or (19)) and resulting contaminants mass flux back to each model. This organization was identical to an explicit evaluation of the Fourier boundary condition in GWM and RM. However, such an explicit evaluation can cause instabilities in GWM, and the stability criterion is very restrictive. Consequently, the organization of data exchange has been reviewed and modified to use an implicit evaluation of the Fourier boundary condition in GWM: (1) computed water levels and solute contaminants concentrations are sent by RM to the junction, (2) after spatial and time interpolations the junction sends the water levels in the river to GWM, and (3) after the flow equation has been solved in GWM the junction receives the calculated water flux and sends resulting contaminants mass flux back to each model. It is assumed that the diffusive solute exchange is negligible compared to advection. Initial results with a junction between just the RM and the GWM (no ocean influence) are given by *Carabin et al.* [1998].

It must be noted that (18) and (19) expressed in terms of water levels must be used with a correction when high salt concentrations are observed in the river. In such a case, we use H_g for equivalent freshwater piezometric head and H_r for water level in the river expressed in terms of equivalent freshwater level:

$$H_r = l_{rb} + (\rho_r/\rho_0) L_{wr} \tag{20}$$

where ρ_r is average density of the river water $[M/L^3]$ and L_{wr} is depth of water in the river $[L]$.

4. Numerical Approach and SUFT3D Background

The GWM code, SUFT3D, was developed at the Laboratoires de Géologie de l'Ingénieur d'Hydrogéologie et de Prospections Géophysiques (LGIH) at the University of Liège. It can treat full 3-D cases under steady or transient conditions for confined or unconfined aquifers. This finite element code solves for groundwater flow, which can be density dependent, and transport of a dissolved contaminant through saturated and unsaturated porous media. Linear interpolation functions are used in elements of eight, six, or four nodes.

The groundwater flow equation solved by SUFT3D is (9), neglecting the solute concentration time variation [*Dassargues*, 1994]. The main flow variable is equivalent freshwater pressure head h. It is well known that this pressure head formulation can cause problems in mass conservation when part of the unsaturated zone is modeled explicitly in the groundwater model [*Milly*, 1985]. Problems stem from inadequate estimates of the generalized storage coefficient. In a partially saturated zone this term is highly nonlinear when applying the mass balance equation over the discretized domain. To solve mass conservation problems in the unsaturated zone, the mixed formulation proposed by *Celia et al.* [1990] (water content and pressure head) is used in the flow equation. Velocity is calculated by directly applying the finite element method to Darcy's equation [*Yeh*, 1981], and in this case, it does not result from the computed pressure field derivatives. This method reduces errors in the mass balance. In addition, it seems to be particularly convenient to simulate density dependent groundwater flow when the vertical component of the velocity can be nonnegligible as in water table aquifers [*Strobl and Yeh*, 1994].

The transport equation solved by SUFT3D can be more complex than (10). Linear degradation, adsorption (with linear, Langmuir, or Freundlich isotherm), and immobile water effect [*Biver et al.*, 1995] are the additional transport processes which can be represented. They are not described in section 2 as they are usually neglected in numerical simulations of saltwater intrusion. The main transport variable is solute concentration (M/L^3) in mobile water. The concentration in immobile water is determined by an analytical solution at each time step [*Biver*, 1993; *Brouyère et al.*, 1997].

The coupled flow and transport equations are solved iteratively (Picard's method). A traditional Galerkin finite element method is used. For the transport equation an Eulerian upstream (EUM) or hybrid Eulerian-Lagrangian (HELM) finite element method [*Yeh*, 1993] can be used for high Peclet numbers (<10 with EUM and unlimited with HELM) and high Courant numbers (only HELM). However, to date, HELM is only available in SUFT3D with hexahedral finite elements.

The well-known WATSOLV solver package [*VanderKwaak et al.*, 1997] is used to ensure effectiveness and reliability.

WATSOLV uses an iterative solving method preconditioned using an incomplete lower-upper factorization. WATSOLV's advantages are (1) its effective sparse storage scheme, (2) the used incomplete factorization method avoiding inverting the entire coefficient matrix, and (3) the iterative process being accelerated using one of two algorithms designed for nonsymmetric coefficient matrices: Generalised Minimal Residual (GMRES) [*Saad and Schultz*, 1986] or Biconjugate Gradient Stabilised (Bi-CGSTAB) [*Van der Vost*, 1992].

Table 1. Case 1 Parameter Values

Parameter	Value
Density difference ratio $\equiv \varepsilon$ in (12)	0.025
Horizontal hydraulic conductivity	4 m/d
Vertical hydraulic conductivity	0.4 m/d
Effective porosity	0.25
Longitudinal dispersivity	10 m
Transverse dispersivity	5 m

Huyakorn et al. [1987].

5. Test Results

Tests were made to check the effectiveness and accuracy of SUFT3D with the latest implementations needed for the SALMON project. They concern principally the resolution of the flow-transport coupled problem in typical situations of seawater intrusion and addition of groundwater-river interaction effects. *Konikow et al.* [1996] reported that for this type of complex coupled problem it was not possible to develop an analytical solution, typically the best means of comparison for evaluating numerical model accuracy. Consequently, SUFT3D was tested on different literature cases, for example, those of *Henry* [1964] and *Huyakorn et al.* [1987]. Gradually, more complex situations were modeled to prepare the work as it fit the SALMON project scope.

5.1. Exchanges With the Ocean

Henry's [1964] is a classical test used to check a code's ability to accurately solve the coupled problem of density-driven flow and transport. *Dassargues* [1994] published comparisons between computed results from SUFT3D and other results for this classical test. A good agreement between the different compared numerical solutions occurred. Now, more realistic conditions have been tested with SUFT3D, with each step increasingly complex.

5.1.1. Unconfined aquifer: Case 1. *Huyakorn et al.* [1987] proposed a test problem for seawater intrusion in an unconfined aquifer. Data, parameters, and boundary conditions of the model domain are in Figure 1 and Table 1. The saltwater boundary is on the left side, and seawater intrusion occurs due to the density effect. Freshwater inflow occurs on the right side. The vertical recharge that occurs to the top of the aquifer is the main difference from the results of *Henry* [1964].

Computed results from SUFT3D were compared with those of *Huyakorn et al.* [1987], *Galeati et al.* [1992], and *Strobl and Yeh* [1994] (Figure 2). Good agreement occurred for the computed isochlor $C_r = 0.5$ (relative concentration) except for that of *Huyakorn et al.* [1987]. However, *Strobl and Yeh* [1994] demonstrated that Huyakorn et al.'s approach was too coarse to achieve the accuracy needed in nodal velocities. Other small observed differences are believed to result from the different solving methods, meshes, and interpolation schemes.

Larger differences observed in the upper part of the domain compared to the results of *Galeati et al.* [1992] are due to dissimilar top boundary conditions. They chose a Dirichlet boundary condition for transport ($C = 0$). We believe that the concentration must not be fixed. While the isochlor $C = 0.5$ remains unchanged, isochlors $C = 0.1$ and $C = 0.3$ are affected by the boundary condition choice (Figure 3). On the top boundary it appears that this condition for transport ($C = 0$) does not represent actual situations where unconfined brackish aquifers are recharged by freshwater. Recharge causes freshwater mixing in the groundwater. This does not mean that the relative salt concentration in the aquifer is zero near the top boundary. The boundary condition proposed by *Huyakorn et al.* [1987] (Figure 1) is more appropriate: in this instance, mass fluxes are equal to advective fluxes when the flow enters the domain with a concentration C^*:

$$\mathbf{n} \cdot [\theta \mathbf{v} C - \theta \mathrm{Dgrad}(C)] = \mathbf{n} \cdot \theta \mathbf{v} C^* = q_n C^* \quad (21)$$

where $\mathbf{n}$ is outward unit vector normal to the boundary [dimensionless] and q_n is normal groundwater flux (equal to the prescribed recharge in our case) $[L/T]$. This boundary condition is closer to reality and was adopted to define the unconfined aquifer top boundary condition in all our simulations.

5.1.2. Large-scale homogeneous aquifer: Case 2. Broader and more complex boundaries have to be considered for exchanges with the ocean model (OM). An aquifer that can be part of the continental shelf has to be considered. As a first step, homogeneous conditions were chosen. Case 2 model dimensions and boundary conditions are in Figure 4 and parameter values are as for case 1 (Table 1). No freshwater input is imposed on the left boundary because the aquifer is supposedly in piezometric equilibrium with the outside conditions.

Case 1 results showed a diffusive-dispersive front of salt water of <100 m. Similar hydrogeologic parameters in case 2 required elements be no larger than 50 m in order to accurately represent the saltwater front. If larger elements had been cho-

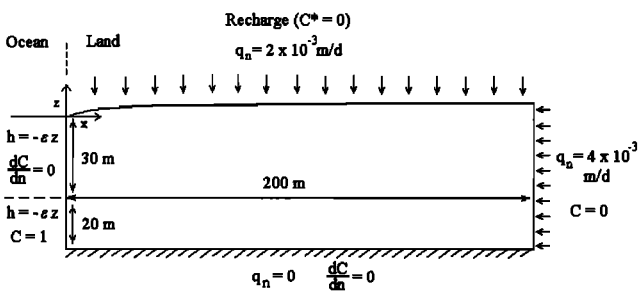

Figure 1. Case 1 definition: seawater intrusion problem of *Huyakorn et al.* [1987].

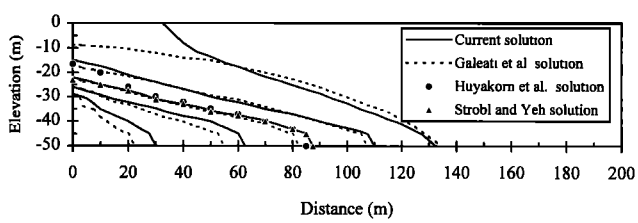

Figure 2. Comparison of results (isochlors 0.1, 0.3, 0.5, 0.7, 0.9) for case 1.

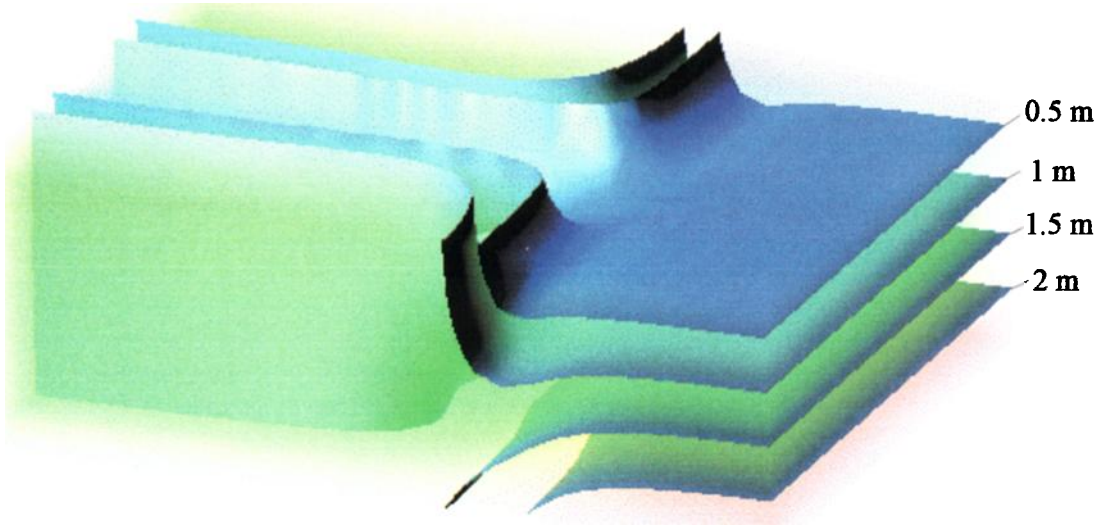

Plate 1. SUFT3D flow results for case 4: isopiezometric surface in equivalent freshwater head.

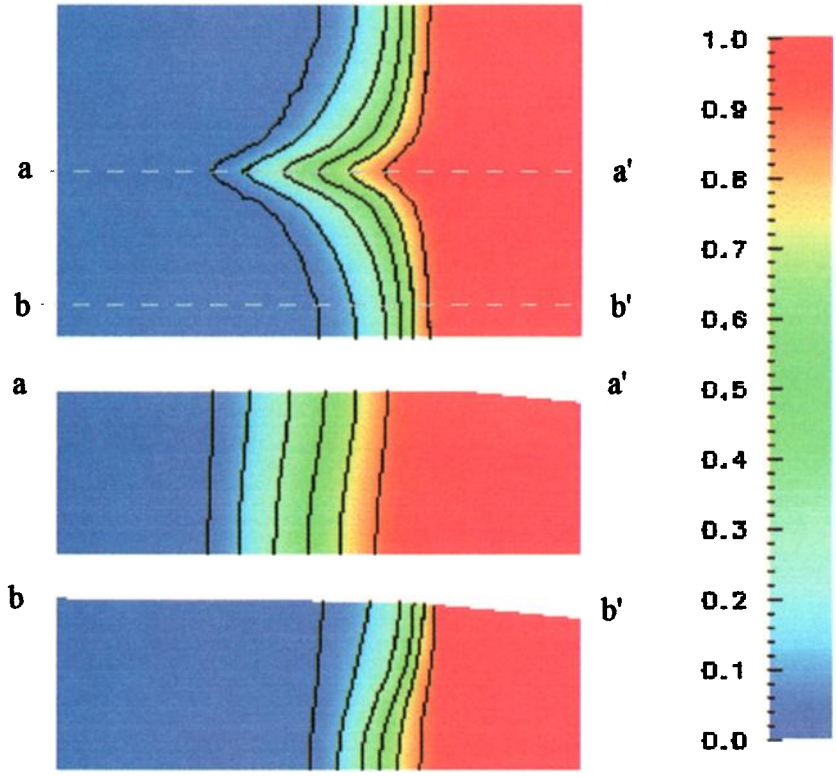

Plate 2. SUFT3D transport results for case 4 (isochlors 0.01, 0.1, 0.3, 0.5, 0.7, 0.9) in plan view at −50 m and vertically in two longitudinal cross sections (a-a′ and b-b′).

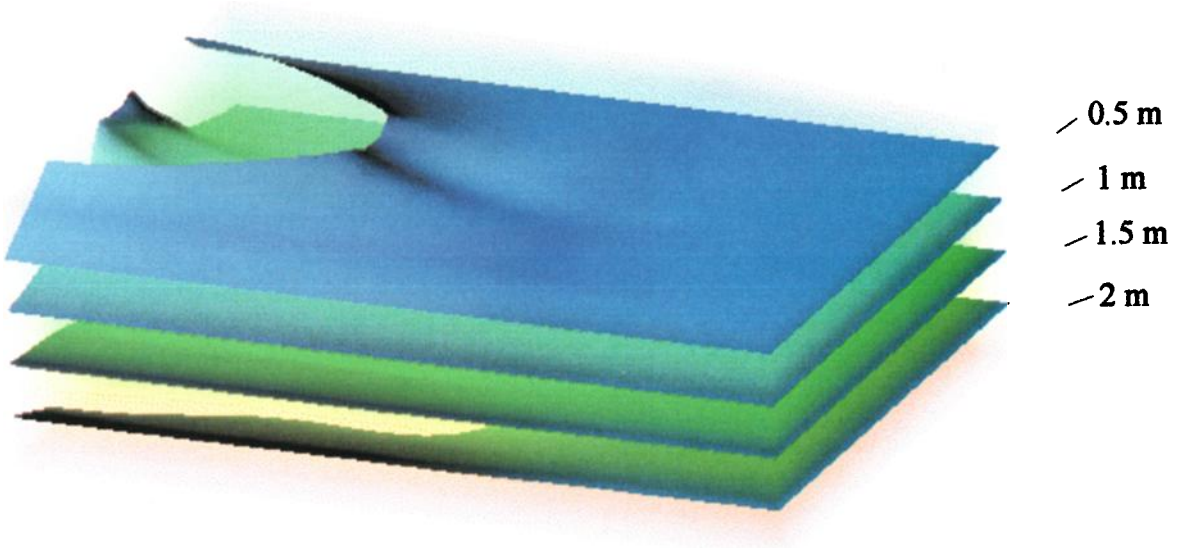

Plate 3. SUFT3D flow results for case 5: isopiezometric surface (equivalent freshwater head).

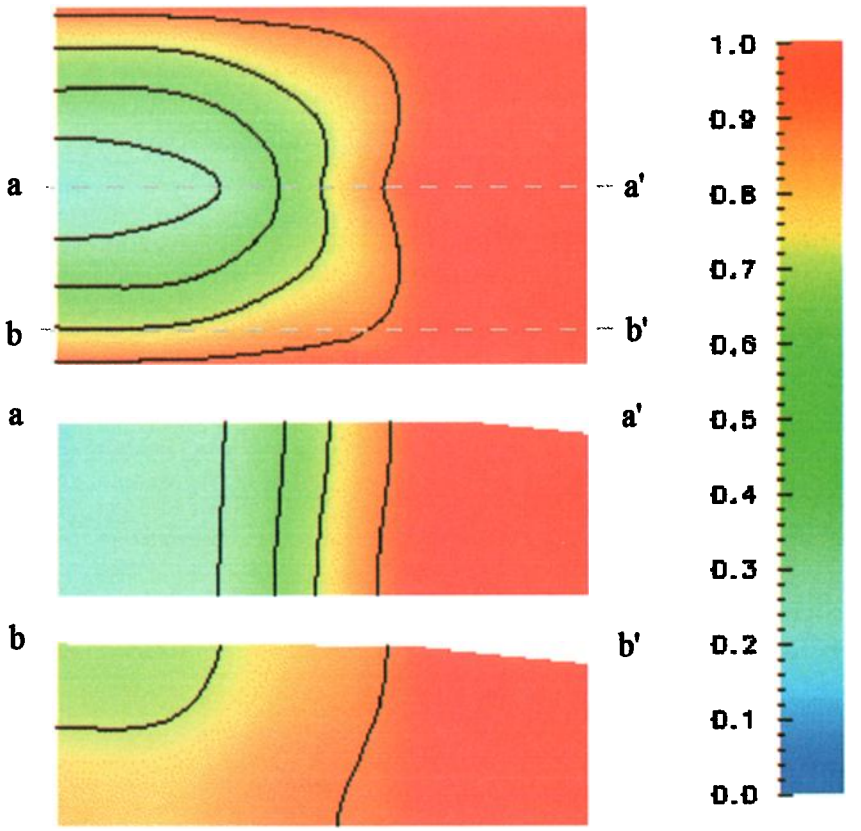

Plate 4. SUFT3D transport results for case 5 (isochlors 0.3, 0.5, 0.7, 0.9) in a horizontal cross section (at −50 m) and two vertical cross sections (a-a′ and b-b′).

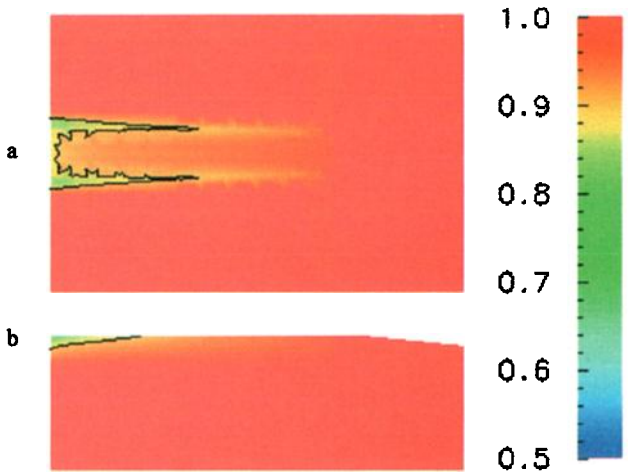

Plate 5. SUFT3D transport results for transient case 1 after 6 months (0.05% river gradient) (a) in plan view at −10 m and (b) vertically along the length of the river: isochlor 0.9.

sen, numerical dispersion would have appeared inducing an enlarged, compared to the actual saltwater front. Such an effect is in the work by *Holzbecher and Baumann* [1994]. To ensure reliable results, spatial discretization must be chosen relative to the modeled phenomenon scale. To maintain the same dispersion value as in case 1, the total number of elements needed to be increased to avoid numerical dispersion since the domain was large.

The intrusion of salt water computed for case 2 is shown in Figure 5. The simulated dispersive front is similar to case 1. A comparison is valid because the computed freshwater inflow 200 m from the coast boundary is nearly equivalent to the freshwater inflow prescribed in case 1. However, seawater intrusion is more important in case 2 because of a 100 m, rather than 50 m, thickness in case 1. Another fundamental difference is that the piezometric head is no longer prescribed with a unit relative concentration at the coastline. This problem arises in all models dealing with seawater intrusion. Relative concentration varies at the boundary which influences the prescribed

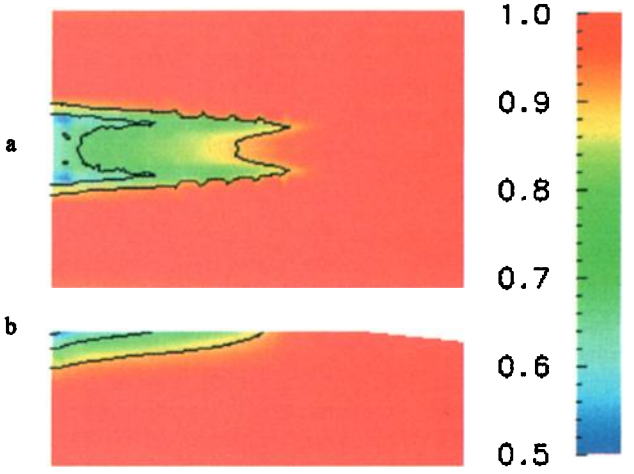

Plate 6. SUFT3D transport results for the transient case 2 after 6 months (0.2% river gradient) (a) in plan view at −10 m and (b) vertically along the length of the river: isochlors 0.5, 0.7, 0.9.

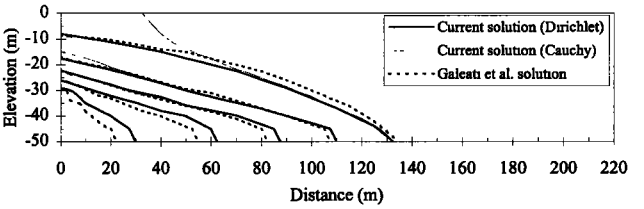

Figure 3. Comparison of results (isochlors 0.1, 0.3, 0.5, 0.7, 0.9) for case 1 with different transport boundary conditions on the top.

pressure head, but the head is dependent on the density and therefore the concentration. In case 2 this problem is moved out to the continental shelf, and thus the pressure head decreases faster upgradient under the coastline. This explains why the dispersive front appears lower at this location.

For transport, Dirichlet conditions ($C = C^*$) cannot be prescribed for the entire continental shelf. To allow freshwater outflow, Neumann condition for transport ($dC/dn = 0$) must be prescribed to a part of the shelf, as was considered for case 1.

5.1.3. Large-scale heterogeneous aquifer: Case 3. Case 3 is the same domain as case 2 but includes a less permeable horizontal layer (aquitard) separating two aquifers. As the contrast in hydraulic conductivity increases between the aquifer and aquitard, the groundwater flow and transport behavior in the upper unconfined and lower confined aquifers become more independent. Thus unconfined and confined conditions are studied in the same domain. Data, parameters, and boundary conditions are in Figure 6 and Table 2. The aquifer parameters are the same as in case 2. Horizontal and vertical hydraulic conductivity values of the less permeable layer are 0.015 times that of the two aquifers. Only the effective porosity was changed to 0.15 instead of 0.25 used for the aquifer. Results show that freshwater concentrations extend farther under the ocean in the lower aquifer (Figure 7). This is because piezometric heads do not decrease as sharply as in the unconfined aquifer. The hydraulic conductivity ratio between the semipervious layer and the aquifers is not small enough to completely prevent interaction between the two aquifers. Consequently, saltwater intrusion in the unconfined aquifer is influenced by the lower aquifer.

5.2. Exchange With Both the Ocean and River

The effectiveness of the river boundary condition in the GWM was also checked. Two cases were previously tested: (1) an alluvial aquifer drained by rivers, including simulation of

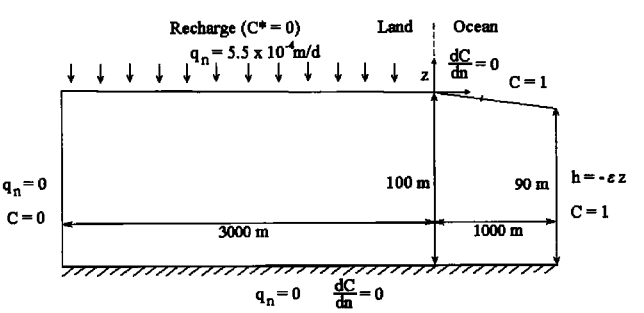

Figure 4. Case 2 definition: seawater intrusion in a large-scale homogeneous aquifer.

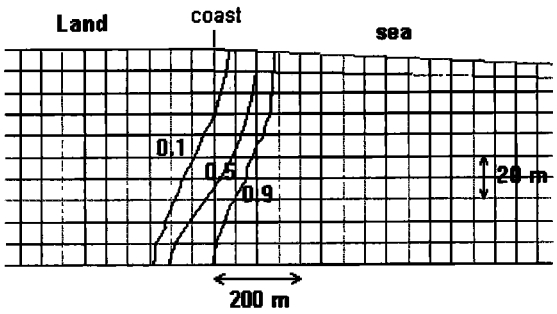

Figure 5. Detailed view of case 2 SUFT3D transport results.

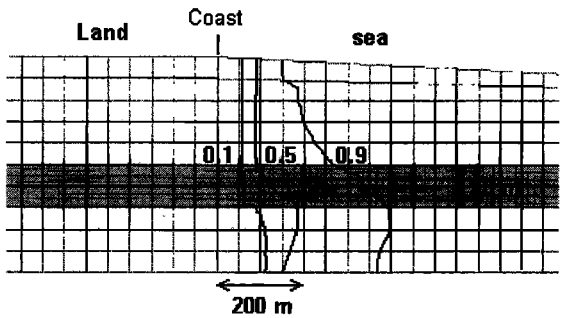

Figure 7. Detailed view of case 3 SUFT3D transport results.

solute mass transfer from the aquifer to the rivers or the contrary, and (2) a pumping well located near a river, creating drawdown and inducing fluxes (i.e., water and solute fluxes) from the river. Results of the tests are given by *Nihoul et al.* [1996]. In the following, only cases involving exchange with both the ocean and river are described.

5.2.1. Aquifer drained by a river: Case 4. The case domain is 3 km long (2 km inland and 1 km under ocean), 2 km wide, and 0.1 km thick with a 300 m wide river in the middle. A finite element mesh network has 100 × 100 × 10 m basic elements, for a total of 8320 elements and 9735 nodes. The mesh in Figure 8 is dark shading where elements contact the ocean and open where they contact river. Data, parameters, and boundary conditions are in Table 3.

Lateral domain boundaries were made impervious because the effects of river draining the aquifer are assumed negligible at that distance and, consequently, groundwater flow would be parallel to those boundaries. The other boundary conditions are similar to case 2 (Figure 4). No flux is imposed on the upgradient (left) boundary (2 km inland) because the aquifer is supposed to be in piezometric equilibrium with the river (which has a low gradient). Under these conditions the only water flux from the aquifer to the draining river can be considered orthogonal to the river and thus parallel to the upgradient boundary.

Results of SUFT3D flow and transport computations are in Plates 1 and 2, respectively. The river drains the aquifer, and consequently, the isopiezometric surfaces (in equivalent freshwater head) are approximately vertical and parallel to the river direction where the ocean is too far away to have an influence on groundwater flow. Approaching the ocean, the isopiezometric surfaces become progressively more horizontal and parallel to the coastline due to the saltwater density effect. Near the river, the localized decrease in piezometric head induced by river drainage increases saltwater intrusion under the river and at the river mouth. Vertically, the computed isochlor $C = 0.5$ is 500 m inland under the river and 100 m inland further from the river (Plate 2). Saltwater intrusion under the river is limited due to fresh groundwater flowing laterally toward the river, draining the aquifer.

5.2.2. Aquifer recharged by a river: Case 5. The same mesh is used as in case 4. Simulations were performed with lower vertical infiltration and the river recharging the aquifer with fresh water. Data, parameters, and boundary conditions are in Table 4. The lateral boundary conditions had to be chosen differently from case 4 (impervious boundaries) because water coming into the domain may also leave through the lateral boundaries. Farther from the river, the aquifer is now assumed to be totally filled with seawater. Thus piezometric heads that take into account the density effect are assigned to lateral boundaries. For transport, a relative concentration of 1 was assigned from the bottom at −100 m to −60 m. Neumann boundary conditions were assigned to the upper part of lateral boundaries. In this manner, fresh water coming from the recharge and mixing with the salty groundwater can flow out of the domain through the upper part. As in case 4, no flux is imposed at the upgradient (left) boundary (2 km inland) because a low gradient is assumed in the recharging river. In this case, the water flux from the river into the aquifer is mainly orthogonal to the river so that it is parallel to the upgradient domain boundary.

The steady state results are in Plates 3 and 4. Fresh water from the river recharges the aquifer filled with seawater. Consequently, initial horizontal isopiezometric surfaces are modified by this input. The recharge is effective only where river water levels become higher than the equivalent freshwater piezometric heads in the aquifer (because fresh water is supposed in the river). The resulting groundwater flow pattern is

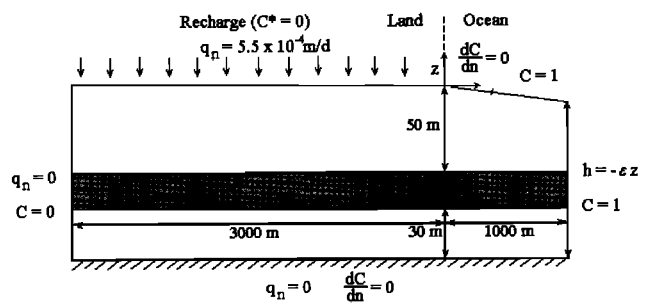

Figure 6. Case 3 definition: seawater intrusion in a large-scale heterogeneous aquifer.

Table 2. Case 3 Parameter Values for Large-Scale Heterogeneous Aquifer Environment

Parameter	Value
Density difference ratio ≡ ε in (12)	0.025
Horizontal hydraulic conductivity	4 m/d
Vertical hydraulic conductivity	0.4 m/d
Effective porosity	0.25
Horizontal hydraulic conductivity in the aquitard	0.06 m/d
Vertical hydraulic conductivity in the aquitard	0.006 m/d
Effective porosity in the aquitard	0.15
Longitudinal dispersivity	10 m
Transverse dispersivity	5 m

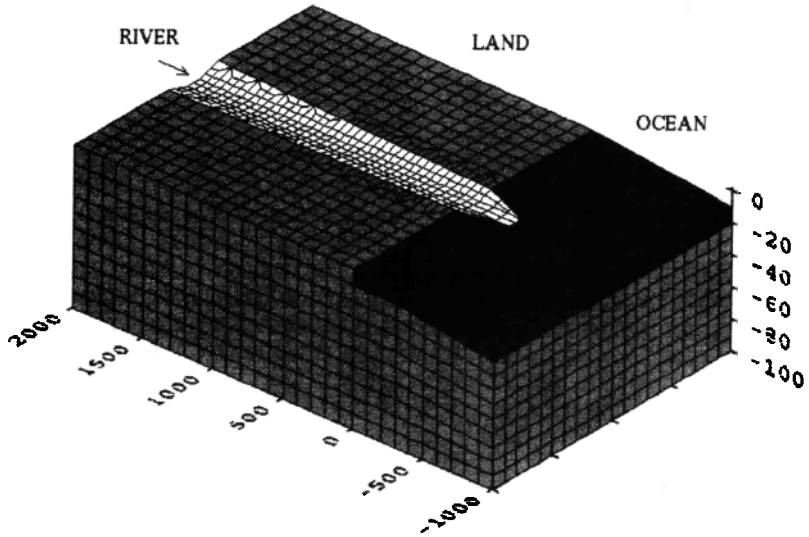

Figure 8. Case 4 and 5 definition: simultaneous groundwater-river and groundwater-seawater interaction.

more complex than case 4 because the density effect has an influence over the entire domain. At depth (Plate 3), flux of salt water coming from the lateral boundaries and the ocean converge under the river where the pressure head is decreased by the freshwater input in the aquifer. In the upper part, groundwater flux is inverted and directed out of the domain through the lateral boundaries and the downstream part of the river. The outgoing groundwater salt concentration is high ($C_r \cong 0.9$). It comes from the deepest part and is only partially mixed with fresh water from the river. Consequently, freshwater input from the river principally modifies the relative concentration under the river and in the upper aquifer part.

After a long drought, rainfall in upstream regions brings fresh water toward the ocean via the rivers. A simulation was done to illustrate river-aquifer exchange transient behavior. Parameters and boundary conditions from case 5 were used. For initial conditions it was assumed that the drought period had resulted in extensive aquifer water level drawdown and complete seawater intrusion. Consequently, an initial concentration of $C_r = 1$ is throughout the aquifer. The initial gradient in the river is assumed to be negligible. For 10 days we simulated a river gradient increase from 0 to 0.05% maintained constant thereafter. Simulation results after 6 months (Plate 5) shows that fresh water flowing from the river does not significantly ($C_r > 0.8$) decrease the aquifer salt concentration. The river gradient is therefore not the only influencing parameter. Hydraulic conductivity and transfer coefficient (K_r/e_r) also influence the results. The river gradient was then increased to 0.2 from 0.05%. After 6 months the relative concentration under the river (Plate 6) decreased to a C_r below 0.5. For both transient cases, freshwater input is more important through the lateral river boundaries than through the river bottom.

6. Conclusions

In the first stage of the SALMON project, different tests have allowed us to check the groundwater model's ability to be connected to both the ocean and river models. The tests were done with increasingly complex hydraulic and transport conditions approaching realistic situations: confined and unconfined aquifers, local and regional domains, homogeneous and heterogeneous aquifers, influence of river interaction on seawater intrusion, steady and transient cases. Not all results could be compared with analytical solutions or published numerical results. However, where they could, the effectiveness and the reliability of the SUFT3D code were demonstrated. Other tests provided results that seemed logical given the physics of the new problems being evaluated. Results of our innovative tests simulating groundwater exchange with both the river and ocean are particularly useful in understanding the flow-transport dynamics in groundwater systems of the coastal

Table 3. Case 4 Parameter Values for River Draining the Aquifer

Parameter	Value
Fresh water recharge at the top	0.00055 m/d
River bottom transfer coefficient (K_r/e_r)	0.1 d^{-1}
River gradient	0.01%
Density difference, ratio $\equiv \varepsilon$ in (12)	0.025
Horizontal hydraulic conductivity	2 m/d
Vertical hydraulic conductivity	0.2 m/d
Effective porosity	0.15
Longitudinal dispersivity	20 m
Transverse dispersivity	10 m

Table 4. Case 5 Parameter Values for River Recharging the Aquifer

Parameter	Value
Fresh water recharge at the top	0.000035 m/d
River bottom transfer coefficient (K_r/e_r)	0.1 d−1
River gradient	0.05%
Density difference ratio $\equiv \varepsilon$ in (12)	0.025
Horizontal hydraulic conductivity	2 m/d
Vertical hydraulic conductivity	0.2 m/d
Effective porosity	0.15
Longitudinal dispersivity	20 m
Transverse dispersivity	10 m

zones. This is especially true when groundwater-river interactions are taken into account. The two opposite situations of a draining or recharging river have been successfully evaluated.

We have now shown how SUFT3D was prepared to solve practical problems including interaction with both the ocean and the river. As a part of the SALMON project, the groundwater model SUFT3D has been connected to the ocean and river models through junctions described by *Ghiot et al.* [1998].

Acknowledgments. As part of the SALMON project, the IBM International Foundation provided hardware support to the Laboratoires de Géologie de l'Ingénieur, d'Hydrogéologie et de Prospections Géophysiques of the University of Liège and provided the IBM Visualisation Data Explorer program V1.2. Thanks to this support, the SUFT3D program is being developed in an IBM Risc System/6000 environment and results are able to be postprocessed by Data Explorer. Concepts about groundwater-river interactions are also developed within the research project "Integrated modeling of the hydrological cycle in relation to global climate changes," supported by Prime Minister's Office, Federal Office for Scientific, Technical and Cultural Affairs of Belgium in the scope of the general program "Global Change Sustainable Development." We thanks also Keith Kennedy for helping us in the English redaction.

References

Bear, J., and Y. Bachmat, *Introduction to Modeling of Transport Phenomena in Porous Media*, 553 pp., Kluwer Acad., Norwell, Mass., 1990.

Bear, J., and A. Verruijt, *Modeling Groundwater Flow and Pollution*, 414 pp., D. Reidel, Norwell, Mass., 1987.

Beckers, J. M., Application of a 3D model to the western Mediterranean, *J. Mar. Syst.*, *1*, 315–332, 1991.

Biver, P., Etude phénoménologique et numérique de la propagation de polluants miscibles dans un milieu à porosité multiple, Ph.D. thesis, 389 pp., Fac. of Appl. Sci., Univ. of Liège, Liège, Belgium, 1993.

Biver, P., V. Hallet, and A. Dassargues, Contribution to the simulation of nitrates transport in a double-porosity aquifer, paper presented at Solution '95, XXVI International Congress, Int. Assoc. of Hydrol. Sci., Alberta, Canada, 1995.

Brouyère, S., V. Hallet, and A. Dassargues, Effet de retard et de piégeage des polluants dus à la présence d'eau immobile dans le milieu souterrain: Importance de ces effets et modélisation, paper presented at National Colloquium, Comité Belge de Géol. de l'Ing., Leuven, Belgium, 1997.

Carabin, G., A. Dassargues, and S. Brouyère, 3D flow and transport groundwater modelling including river interactions, in *Computational Methods in Water Resources XII*, vol. 1, edited by V. N. Burganos et al., Comput. Mech., Boston, Mass., pp. 569–576, 1998.

Celia, M. A., E. T. Bouloutas, and R. L. Zarba, A general mass-conservative numerical solution for the unsaturated flow equation, *Water Resour. Res.*, *26*(7), 1483–1496, 1990.

Dassargues, A., Validation of a finite element code to simulate the coupled problem of salt transport in groundwater, in *Computer Techniques in Environmental Studies V, Proceedings of ENVIROSOFT'94, San Francisco*, vol. 1, pp. 173–180, Comput. Mech., Boston, Mass., 1994.

Dassargues, A., S. Brouyère, G. Carabin, and F. Schmitz, Conceptual and computational challenges when coupling a groundwater model with ocean and river models, in *Computational Methods in Water Resources XI*, vol. 1, edited by A. A. Aldama et al., pp. 77–84, Comput. Mech., Boston, Mass., 1996.

Essaid, H. I., A multilayered sharp interface model of coupled freshwater and saltwater in coastal systems: Model development and application, *Water Resour. Res.*, *26*(7), 1431–1454, 1990.

Galeati, G., G. Gambolati, and P. S. Neuman, Coupled and partially coupled Eulerian-Lagrangian model of freshwater-seawater mixing, *Water Resour. Res.*, *28*(1), 149–165, 1992.

Gartling, D. K., and C. E. Hickox, A numerical study of the applicability of the Boussinesq approximation for fluid-saturated porous media, *Int. J. Numer. Methods Fluids*, *5*, 995–1013, 1985.

Ghiot, C., P. Bauler, J. M. Beckers, G. Carabin, A. Dassargues, E. Delhez, J. F. Deliège, and E. Everbecq, Sea Air Land Modelling Operational Network, in *Hydroinformatics 98*, edited by V. Babovic and L. C. Larsen, pp. 371–377, A. A. Balkema, Rotterdam, Netherlands, 1998.

Hassanizadeh, S. N., and T. Leijnse, On the modeling of brine transport in porous media, *Water Resour. Res.*, *24*(3), 321–330, 1988.

Henry, H. R., Effects of dispersion on salt encroachment in coastal aquifer, in *Sea Water in Coastal Aquifer, U.S. Geol. Surv. Water Supply Pap.*, *1613-C*, 70–84, 1964.

Hillel, D., *Soil and Water: Physical Principles and Processes*, Academic, San Diego, Calif., 1984.

Holzebecher, E., and R. Baumann, Numerical simulations of seawater intrusion into the Nile delta aquifer, in *Computational Methods in Water Resources X*, vol. 2, edited by A. Peters et al., pp. 1011–1018, Kluwer Acad., Norwell, Mass., 1994.

Huyakorn, P. S., and G. F. Pinder, *Computational Methods in Subsurface Flow*, 473 pp., Academic, San Diego, Calif., 1983.

Huyakorn, P. S., P. F. Andersen, J. W. Mercer, and H. O. White, Saltwater intrusion in aquifers: Development and testing of a three-dimensional finite element model, *Water Resour. Res.*, *23*(2), 293–312, 1987.

Kinzelbach, W., *Groundwater Modelling*, 333 pp., Elsevier, New York, 1986.

Kipp, K. L., Jr., HST3D: A computer code for simulation of heat and solute transport in three dimensional groundwater flow systems, *U.S. Geol. Surv. Water Resour. Invest. Rep.*, *86–4095*, 510 pp., 1987.

Konikow, L. F., P. J. Campbell, and W. E. Sanford, Modelling brine transport in a porous medium: A re-evaluation of the HYDROCOIN level 1 case 5 problem, in *Calibration and Reliability in Groundwater Modelling, Proceedings of ModelCARE 96, IAHS Publ.*, *237*, 363–372, 1996.

Larabi, A., and F. De Smedt, Three dimensional finite element model for saltwater intrusion into aquifer, in *Computational Methods in Water Resources X*, vol. 2, edited by A. A. Aldama et al., pp. 1019–1026, Kluwer Acad., Norwell, Mass., 1994.

Liu, P. L. F., A. H. D. Cheng, J. A. Ligget, and J. H. Lee, Boundary integral equation solutions of moving interface between two fluids in porous media, *Water Resour. Res.*, *17*(5), 1445–1452, 1981.

McDonald, M. G., and A. W. Harbaugh, A modular three-dimensional finite-difference groundwater flow model, *U.S. Geol. Surv., Tech. Water Resour. Invest.*, *6*(A1), 548 pp., 1988.

Milly, P. C. D., A mass-conservative procedure for time-stepping in models of unsaturated flow, *Adv. Water Resour.*, *8*, 32–36, 1985.

Munhoven, S., Modélisation d'un aquifère salé, Grad. thesis, 141 pp., Fac. of Appl. Sci., Univ. of Liège, Belgium, 1992.

Nawalany, M., Combining the analytical and finite element models of the river-groundwater interaction, in *Computational Methods in Water Resources X*, vol. 1, edited by A. A. Aldama et al., pp. 83–90, Kluwer Acad., Norwell, Mass., 1994.

Nihoul, J. C. J., A. Monjoie, J. S. Smitz, J. M. Beckers, A. Dassargues, E. Everbeck, G. Carabin, and J. F. Deliege, Technical report of the SALMON project: An IBM environmental research program, Cent. for Environ. Stud., Univ. of Liège, Belgium, 1996.

Saad, Y., and M. H. Schultz, GMRES: A generalized minimal residual algorithm for solving nonsymmetric linear systems, *SIAM J. Sci. Stat. Comput.*, *7*, 856–869, 1986.

Smitz, J., E. Everbecq, J. F. Deliège, J. P. Descy, R. Wollast, and J. P. Vanderborght, PEGASE: Une méthodologie et un outil de simulation prévisionnelle pour la gestion de la qualité des eaux de surface, *Tribune Eau Belgium*, *588*(4), 73–82, 1997.

Strobl, R. O., and G. T. Yeh, Two-dimensional modelling of salt water intrusion, in *Computational Methods in Water Resources X*, vol. 2, edited by A. A. Aldama et al., pp. 1035–1042, Kluwer Acad., Norwell, Mass., 1994.

Taigbenu, A. E., J. A. Ligget, and A. H. D. Cheng, Boundary integral solution to seawater intrusion into coastal aquifers, *Water Resour. Res.*, *20*(8), 1150–1158, 1984.

VanderKwaak, J. E., P. A. Forsyth, K. T. B. MacQuarrie, and E. A. Sudicky, Watsolv user guide version 2.16, Waterloo Cent. for Groundwater Res., Univ. of Waterloo, Waterloo, Ont., Canada, 1997.

Van der Vorst, H., Bi-CGSTAB: A fast and smoothly converging variant of Bi-CG for the solution of nonsymmetric linear systems, *SIAM J. Sci. Stat. Comput.*, *13*, 631–664, 1992.

Voss, C. I., and W. R. Souza, Variable density flow and solute transport simulation of regional aquifers containing a narrow freshwater-

saltwater transition zone, *Water Resour. Res.*, *23*(10), 1851–1866, 1987.

Yeh, G. T., On the computation of Darcian velocity and mass balance in the finite element modeling of groundwater flow, *Water Resour. Res.*, *17*(5), 1529–1534, 1981.

Yeh, G. T., Application of hybrid Lagrangian-Eulerian finite element approaches to contaminant transport, and, 2DFEMFAT user's manual, Notes and oral communication on modelling of flow and contaminants in the subsoil, chap. 11–12, Int. Ground Water Model. Cent., IHE-Delft, Delft, Netherlands, 1993.

G. Carabin and A. Dassargues, Laboratoires de Géologie de l'Ingénieur, d'Hydrogéologie, et de Prospection Géophysique, Université de Liège, Bat. B19, 4000 Liège, Belgium. (gcarabin@ibm1.lgih.ulg.ac.be; alain.dassargues@geo.kuleuven.ac.be)

(Received June 15, 1998; revised April 9, 1999;
accepted April 13, 1999.)